Zeitschrift: Helvetica Physica Acta
Band: 50 (1977)
Heft: 6

Artikel: Measurement of the polarization parameter in ^+p-scattering at 291.4 and 310.0 MeV
Autor: Dubal, L. / Eaton, G.H. / Frosch, R.
DOI: https://doi.org/10.5169/seals-114892

Helvetica Physica Acta, Vol. 50 (1977), Birkhäuser Verlag, Basel

Measurement of the polarization parameter in π^+p-scattering at 291.4 and 310.0 MeV

by **L. Dubal, G. H. Eaton, R. Frosch, H. Hirschmann, S. Mango, J. McCulloch, R. Minehart,**[1]) **F. Pozar** and **U. Rohrer**

SIN, Villigen, Switzerland

P. Wiederkehr

High Energy Physics Laboratory, ETHZ, Villigen, Switzerland

(25. VII. 1977)

Abstract. The polarization parameter in elastic π^+p scattering has been measured for pion laboratory kinetic energies of 291.4 and 310.0 MeV and for scattering angles from 52° to 145° c.m. The resulting D-wave phase shifts agree with theoretical predictions based on dispersion relations.

1. Introduction

In recent phase shift analyses of pion-proton scattering [1, 2] only a small amount of data was available for the polarization parameter in elastic π^+p scattering at energies up to 310 MeV. This quantity however is useful to improve the precision of the phases of the partial waves with isospin 3/2. As Amsler et al. [3, 4] have demonstrated earlier the error of these phases at energies near the first resonance can be reduced by up to one order of magnitude if polarization data are included in the phase shift analysis.

We now report measurements of the polarization parameter in elastic π^+p scattering at kinetic lab energies of the incident pions of 291.4 MeV and 310.0 MeV. The present work was mainly dedicated to a determination of phase shifts up to the D waves independent of predictions from fixed-t dispersion relations [1, 2] for the D phases.

2. Experimental method

We summarize in the following the main features of our experimental method; further details are discussed in References [3] and [5]. A schematic layout of the apparatus is shown in Figure 1. A polarized proton target was used with the axis of polarization perpendicular to the scattering plane defined by scintillation counters.

[1]) Permanent address: Univ. of Virginia, Charlottesville, VA, USA.

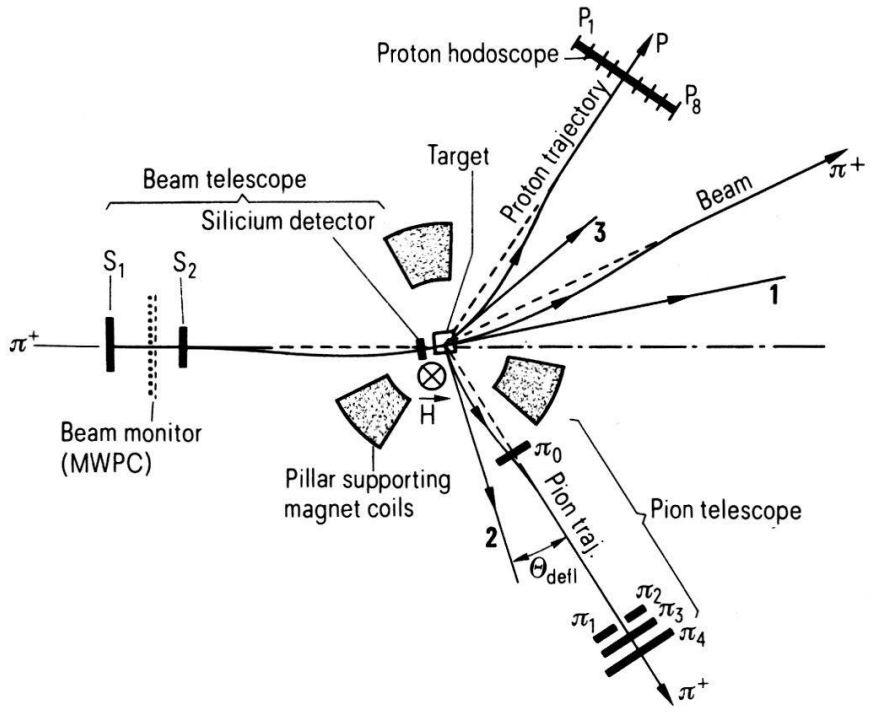

Figure 1
The apparatus (schematic). The particle trajectories in the magnetic field of the polarized target are shown. Lines with numbers 1, 2, 3 indicate the momentum directions at the vertex point of the incident pion, the scattered pion and the recoil proton respectively. Dashed lines indicate the asymptotic directions.

For this geometry the counting rate per unit scattering angle, $n(\theta^*, P_T)$, of pions elastically scattered from polarized protons is given by the expression

$$n(\theta^*, P_T) = n_0(\theta^*) \quad [1 + P(\theta^*)P_T] \tag{1}$$

where θ^* is the scattering angle in the center of mass system, $P(\theta^*)$ is the polarization parameter (P-parameter) and P_T is the polarization of the target, i.e., twice the component of the proton spin along the polarization axis. $n_0(\theta^*)$ is the counting rate at $P_T = 0$. Equation (1) may be derived, e.g., from equation (6) of Reference [6].

In order to determine the P-parameter we measured at fixed energies and several fixed scattering angles the dependence of the rate $n(\theta^*, P_T)$ on the target polarization.

2.1 Target

The polarized target [5] consisted of butanol and was contained in a cubic box with dimensions 1 cm × 1 cm × 1 cm. The butanol pellets were embedded in a He^3-bath at a temperature of 0.5°K. The static magnetic field (perpendicular to the paper plane in Figure 1) of 25 kG was excited by two superconducting Helmholtz coils. The free protons in the butanol were polarized dynamically by applying a 70 GHz high frequency field. Their polarization was measured with the help of a nuclear magnetic resonance method. The absorption of an RF-field at resonance (around 106 MHz) was determined with the target in the dynamically polarized state as well as in the state of polarization in the static magnetic field alone. The polarization of this latter state is given by

$$P_T^{(0)} = \tanh(\mu_p H/kT) \tag{2}$$

where μ_p is the magnetic moment of the proton and H is the magnetic field strength. $P_T^{(0)}$ was used for the calibration of the NMR system. The target polarization was about 65%. It was measured with a relative accuracy of typically 5%. The polarization was reversed by slightly adjusting the magnetic field [5]. The geometrical arrangement of the apparatus and the direction of the magnetic field remained unaltered.

2.2 Particle detection

The particle detection system consisted of counters which registered the incident pions, the scattered pions and the recoil protons. The beam telescope comprised two scintillation counters (S_1, S_2) and, immediately in front of the target, an 8 mm × 8 mm × 1.5 mm (thickness) silicon surface barrier detector, thus keeping all materials with free protons far away from the target region. A multiwire proportional chamber (MWPC) monitored the position and the profile of the incident beam. The scattered pions were detected with a counter telescope ($\pi_0 \cdots \pi_4$) split in two halves, each subtending an angle of 5.7° in the lab-system. A hodoscope consisting of eight counters ($P_1 \cdots P_8$) detected the recoil protons within a total angle of 26° in the laboratory. Both the detectors for the scattered particles as well as the pillars supporting the Helmholtz coils were independently rotatable around the target center in a plane normal to the line of target polarization. Events with a desired center of mass scattering angle were selected by means of the angular position of the pion detector with the proton hodoscope centered on the appropriate recoil direction. The detector positions were corrected for the bending of the particle trajectories (θ_{defl}) in the magnetic field. The total angular resolution of the apparatus was mainly determined by the dimensions of the pion detector and of the target, and was 2.5° to 3.2° in the c.m.s.

During the measurement all events were counted which produced coincident electronic signals from the telescopes for the beam and the scattered pions, and from at least one of the proton counters. Using pulse height and range discrimination we eliminated protons elastically scattered into the pion telescope.

2.3 Beam

We used the SIN πM3 beam of secondary (positive) pions with 2×10^5 to 5×10^5 π^+/sec accepted by the beam telescope. From the data of the beam transport system the mean momentum of the pions was known to $\pm 0.5\%$. An independent determination of the beam momentum was achieved at kinetic pion energies of 236 MeV and 310 MeV by measuring the range of the protons contaminating the beam [5]. The difference between the two results for the mean beam momentum was $(0.1 \pm 0.6)\%$. The momentum bite was 4% (FWHM).

In the measurement of the polarization parameter it is essential that the contribution to the number of scattering processes by contaminating particles be negligibly small. The protons were eliminated from the π^+ beam by the use of a carbon degrader between two bending magnets of the beam transport system and additionally by electronic rejection of large pulses from the counters S_1 and S_2 [5]. The contamination of the beam by positive muons was $(13 \pm 3)\%$ and the contamination by positrons was less than 5%. The differential cross sections of μ^+ and

e^+ on protons at the intermediate angles of this experiment are smaller than the πp cross sections by at least an order of magnitude. Therefore no correction due to these contaminating particles was necessary.

3. Determination of the P-parameter

According to equation (1) the number of pions scattered at a fixed angle depends linearily on the target polarization. Thus the P-parameter can be determined from a straight line fit to the event rate dependence on the target polarization.

3.1 Background subtraction

The strongest error source was a background of coincidences resulting from quasi-elastic and non-elastic reactions of pions with the carbon of the butanol and with materials of the target set up. This background is treated as being independent of target polarization and has been subtracted from all rates. The monitoring of the background was carried out using the proton counter hodoscope. The upper histogram in Figure 2 shows a typical distribution over the 8 counters with a maximum produced by recoil protons from the elastic reaction. To estimate approximately the background without further measurement the flat distribution in the outer channels could have been interpolated below the elastic peak. We preferred however to measure the background explicitly with its angular dependence. For this we replaced the butanol target by an equally dimensioned target consisting of thin graphite bars with a total mass equal to the carbon mass in the butanol. Two further series of measurements, one with the He^3-bath alone instead of the butanol target and one with empty

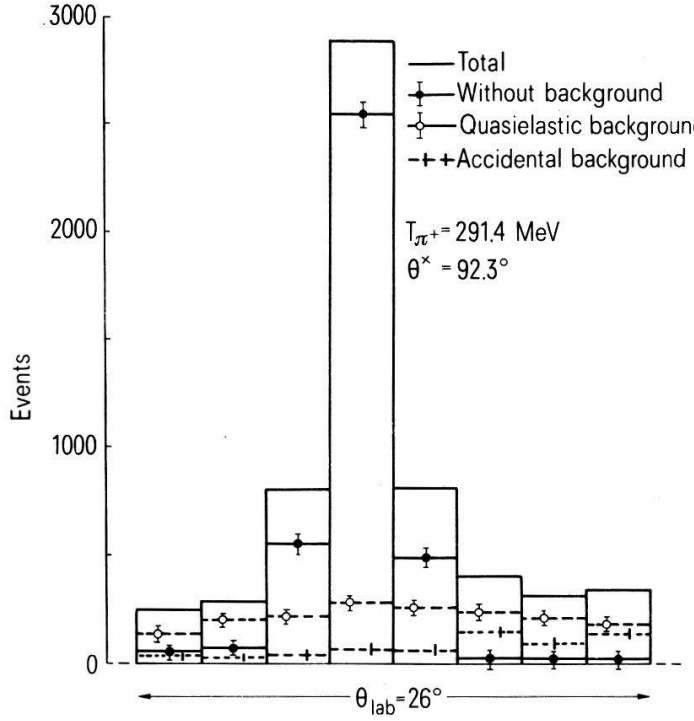

Figure 2
Recoil proton distribution in the hodoscope. Kinetic energy of incident π^+: 291.4 MeV. Scattering angle: 92.3° (c.m.s.).

target, determined the remaining contributions to the background. The dashed line in Figure 2 shows the reconstructed background distribution. The slight curvature is probably due to quasi-elastic processes.

Intensity dependent background. Accidental triple coincidences mainly arose from true double coincidences (beam and scattered pion) with an accidental proton signal and from true coincidences (scattered pion and proton) with an accidental beam signal. The number of accidentals and the corresponding distribution in the proton hodoscope has been reconstructed with standard methods. In the example of Figure 2 the result is represented by the dotted line.

Subtraction of nonelastic background and accidentals from the total rates lead to hodoscope distributions which were almost consistent with zero in the outer channels as shown in Figure 2. We concluded from this that, as expected, only the three counters with the highest rates were hit by elastically scattered protons. The rate of elastic events was therefore calculated by the following procedure: first, all reconstructed background was separately subtracted from each of the 8 hodoscope rates. Then, using the remaining content of the outer channels only, we fitted a straight line below the elastic peak and subtracted there again the interpolated value. Finally, the sum from the three high channels was considered as the elastic rate. The correction calculated with the fitted line was consistent with zero except for the biggest scattering angles, where it still reached 5% of the elastic rate. In these cases we calculated the P-parameter with and without subtraction of this unexplained background in the three central channels. The results for the P-parameter differed by less than 0.01. The subtraction has been applied to all data in Tables 1 and 2.

3.2 *Errors of target polarization measurement*

The target polarization was monitored periodically and kept constant to 5%. In the analysis of the data we used beam-weighted averages. The error due to fluctuations of the polarization was negligible compared with the statistical error from the rates. There was however a systematic uncertainty due to the calibration (see Section 2.1) which lead to a normalization uncertainty for the P-parameter.

3.3 *Results*

The P-parameter has been determined at 14 scattering angles for the kinetic pion energies 291.4 MeV and 310.0 MeV. Results are given in the Tables 1 and 2 and in the Figures 3 and 4. The quoted errors are statistical only.

The data at 291.4 MeV have been taken in several series of measurements with different normalization uncertainties. The averages from data with a normalization uncertainty less than 5% are listed in column I of Table 1 and represented by the full circles in Figure 3. In some measurements the normalization uncertainty was about 10%. The P-parameters from those data are listed in column II of Table 1 and illustrated by the open circles in Figure 3. Results from type I and II data were not averaged but treated separately in the phase shift analysis. At 310.0 MeV the normalization uncertainty was 5%. For comparison Figure 4 shows also the P-parameter values from an earlier measurement [7, 8].

Table 1
Polarization parameter (P) measured at a mean kinetic laboratory energy of the incident pions of (291.4 ± 1.9) MeV. The uncertainty of the mean beam momentum was ±0.5%, the momentum bite of the beam was 4% (FWHM). Quoted uncertainties of P are statistical. P values in columns I and II have different systematic uncertainties (see Section 3.3).

θ^* (degrees)	P I	P II
55.7	0.198 ± 0.023	—
63.4	0.262 ± 0.028	—
81.5	0.335 ± 0.038	0.408 ± 0.025
85.9	0.423 ± 0.024	0.409 ± 0.026
88.3	0.444 ± 0.047	0.452 ± 0.032
92.3	0.448 ± 0.028	0.448 ± 0.038
104.2	0.295 ± 0.037	0.278 ± 0.035
110.0	0.193 ± 0.035	0.137 ± 0.037
116.0	0.023 ± 0.038	0.122 ± 0.031
121.4	0.009 ± 0.039	0.035 ± 0.033
123.9	−0.041 ± 0.040	−0.043 ± 0.032
128.9	−0.096 ± 0.040	−0.052 ± 0.028
140.4	−0.113 ± 0.029	—
145.2	−0.109 ± 0.024	—

Table 2
Polarization parameter measured at a mean kinetic laboratory energy of the incident pions of (310.0 ± 2.0) MeV. For notations, beam properties and quoted uncertainties see Table 1.

θ^* (degrees)	P
51.8	0.181 ± 0.026
59.3	0.238 ± 0.024
69.6	0.245 ± 0.031
76.2	0.245 ± 0.036
85.7	0.390 ± 0.033
91.8	0.338 ± 0.044
108.1	0.198 ± 0.039
113.5	0.058 ± 0.041
120.9	−0.094 ± 0.052
125.9	−0.039 ± 0.043
130.5	−0.112 ± 0.048
135.2	−0.117 ± 0.048
140.6	−0.089 ± 0.048
145.0	−0.110 ± 0.045

The solid curves in Figures 3 and 4 represent the P-parameter computed from our recalculated phase shifts. The dashed curves are the predictions from the phase shifts of Carter et al. [1].

4. Phase shift analysis

Using our results for the P-parameter we have carried out a phases shift analysis in order to determine the phases of the S, P and D partial waves.

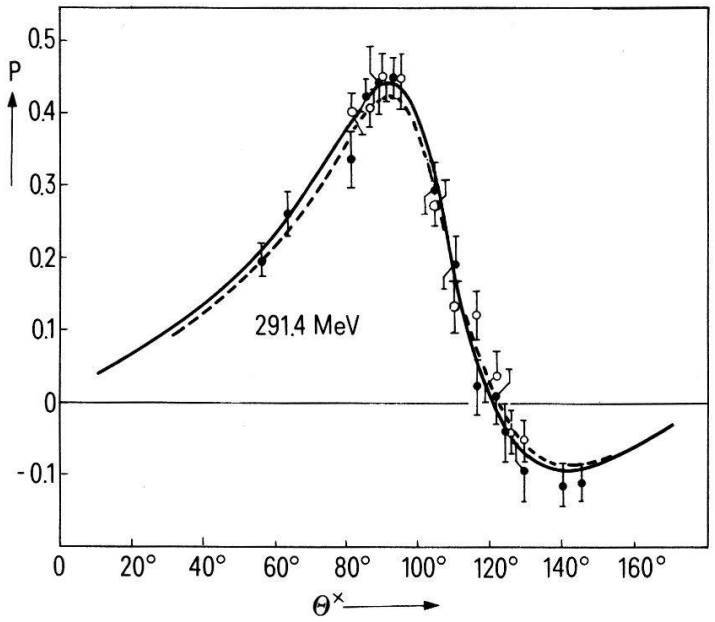

Figure 3
Polarization parameter (P) versus c.m.s. scattering angle (θ^*) at a mean kinetic energy of 291.4 MeV. Quoted errors are statistical. Full circles represent type I data, open circles represent type II data in Table 1. Solid curve: prediction of the P-parameter from the phase shifts recalculated in this work. Dashed curve: prediction from the phase shifts in Reference [1].

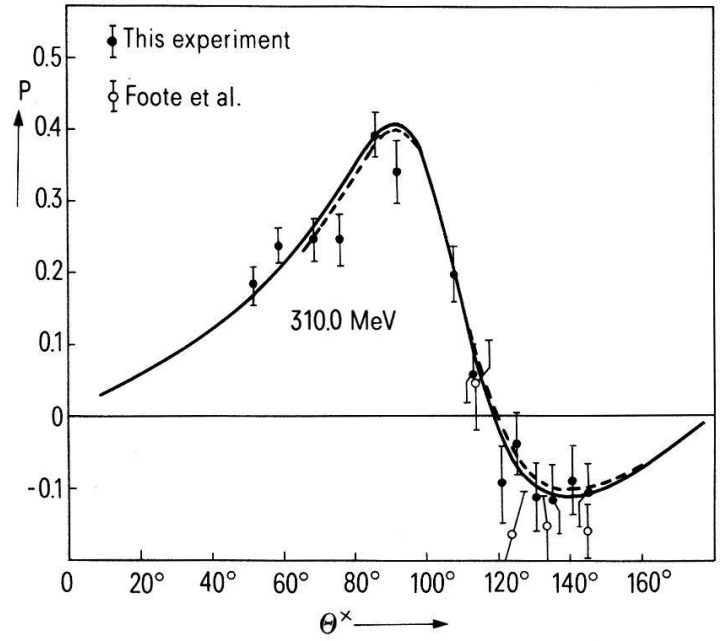

Figure 4
Polarization parameter (P) versus c.m.s. scattering angle (θ^*) at a mean kinetic energy of 310.0 MeV. Full circles: this experiment; quoted errors are statistical. Open circles: results from Reference [7] and [8]. Meaning of the curves as in Figure 3.

The phases were calculated as fitted parameters by minimization of an appropriate chi-square-function. The experimental input applied to this function included our P-parameter data at the mean kinetic energies (291.4 $\pm$ 1.9) MeV and (310.0 $\pm$ 2.0) MeV, differential cross sections at (291.4 $\pm$ 0.96) MeV [9], (292.9 $\pm$ 1.6) MeV [10] and (308.0 $\pm$ 1.6) MeV [10] as well as total cross sections [11, 12] interpolated to the energies of our experiment.

The iterative computation process was started at phase shift values obtained from the analysis of Carter et al. [1]. In this work only the S and P phases were determined directly from experimental data, whilst the phases of higher partial waves were introduced as fixed numbers estimated from dispersion relations and extrapolations. In contrast we only fixed the F phases, taken again from the work of Carter et al. at the following values:

at 291.4 MeV: $\delta(\mathrm{F35}) = 0$; $\delta(\mathrm{F37}) = 0.53°$;
at 310.0 MeV: $\delta(\mathrm{F35}) = 0$; $\delta(\mathrm{F37}) = 0.58°$;

(labelling Fij: $i = 2 \times$ isospin, $j = 2 \times$ angular momentum). All corrections due to absorption were neglected. Electromagnetic effects were treated with a procedure as used in Reference [1]. For the electromagnetic phase shift corrections of S and P waves we inserted the values calculated by Tromborg et al. [13]. No phase shift corrections have been applied to the D phases, since they are expected to be much smaller than the error [14]. Most of the experimental input data sets were multiplied by a normalization factor (a_{fit}) which was fitted together with the phase shifts. Where the systematic uncertainty (Δa) was known a term

$$\left[\frac{1 - a_{\mathrm{fit}}}{\Delta a}\right]^2 \tag{3}$$

was added to the chi-square-function for each factor.

Results. At 291.4 MeV both the cross section data [9] and [10] (at 292.9 MeV) are found to be consistent with our P-parameter measurements. The phases in Table 3, column (b), are our result which simultaneously includes all these data. In column (a) the start values are listed. Normalization factors were fitted to the cross sections [10] with a systematic uncertainty $\Delta a = 4.8\%$ and to the P-parameter values of type I (Table 1, column I) with a systematic uncertainty 5%. For the P-parameter

Table 3
Phase shifts in degrees for laboratory kinetic energies of 291.4 MeV (columns (a), (b)) and 310.0 MeV (columns (c), (d)). Values in columns (a) and (c) are results of Reference [1], the values with an asterisk are estimates based on dispersion relations. Values in columns (b) and (d) are results of our calculations which include P parameter data of this experiment and cross section data of References [9, 10, 11, 12]. The χ^2 values and the degrees of freedom of our fits are also listed.

Partial wave	kinetic energy 291.4 MeV		kinetic energy 310.0 MeV	
	Carter et al. (a)	this Exp. (b)	Carter et al. (c)	this Exp. (d)
$S31$	−20.08 ± 0.36	−20.40 ± 0.23	−20.49 ± 0.50	−20.14 ± 0.49
$P31$	−7.44 ± 0.55	−8.26 ± 0.26	−7.76 ± 0.45	−7.99 ± 0.46
$P33$	133.54 ± 0.29	133.25 ± 0.19	136.75 ± 0.90	136.17 ± 0.47
$D33$	0.25[*]	0.21 ± 0.19	0.25[*]	0.33 ± 0.36
$D35$	−0.91[*]	−0.81 ± 0.18	−1.01[*]	−1.08 ± 0.31
Chi-square	—	51.6	—	20.2
Degrees of freedom	—	47	—	19

values of type II (Table 1, column II) we treated the normalization factor as a completely free parameter, omitting a term of the form (3) in the chi-square function and thus using only the relative dependence of the P-parameter on the scattering angle. The resulting values for a_{fit} differed from 1 by an amount consistent with the estimated uncertainty Δa in all cases.

As a test we allowed the F37 phase to vary also. The fit yielded $\delta(\text{F37}) = (0.21 \pm 0.16)°$, leaving the other phases unchanged within the error limits.

With the P-parameter data at 310 MeV we combined differential cross sections measured at 308 MeV [10]. The start values for the phases and the results are listed in Table 3, columns (c) and (d) respectively. Normalization factors were fitted to the P-parameters and to the cross sections with systematic uncertainties 5% and 4.8% respectively. A computation including cross sections from an earlier measurement [8] did not change the phases significantly from the values listed in Table 3, column (d), but the confidence level of the fit was only 15% in this case.

Conclusions. Within the error limits the recalculated phases at both energies are in agreement with the results of Ref. [1]. The uncertainties of some of the S and P phases have been noticeably reduced by our work. The D phases have been determined experimentally for the first time with significant precision; our D phases agree well with the estimates of Carter et al. [1].

Acknowledgements

The authors wish to thank Prof. D. V. Bugg for private communications and to Prof. G. Rasche for a valuable discussion. We are indebted to G. Buxton, M. Byrne, P. House and B. Jost for help during the running of the experiment, and to H. Lietzow and P. Weymuth for assistance in the operation of the polarized target. The contribution of C. Amsler during the early stages of the experiment is acknowledged. Thanks are due to the many people at SIN whose assistance was invaluable for the completion of the experiment, in particular, to the accelerator crew for their efficient provision of beam.

REFERENCES

[1] J. R. Carter, D. V. Bugg and A. A. Carter, Nucl. Phys. *B58* (1973) 378; for the treatment of the Coulomb corrections in this work see also:
D. V. Bugg, Nucl. Phys. *B58* (1973) 397.
[2] H. Nielsen and G. C. Oades, Nucl. Phys. *B72* (1974) 310.
[3] C. Amsler, F. Rudolf, P. Weymuth, L. Dubal, G. H. Eaton, R. Frosch, S. Mango and F. Pozar, Phys. Lett. *57B* (1975) 289.
[4] C. Amsler, L. Dubal, G. H. Eaton, R. Frosch, S. Mango, F. Pozar and U. Rohrer, Lettere al Nuovo Cim. *15* (1976) 209.
[5] C. Amsler, thesis, ETH Zürich (1975).
[6] O. Chamberlain, E. Segrè, R. D. Tripp, C. Wiegand and T. Ypsilantis, Phys. Rev. *102* (1956) 1659.
[7] J. H. Foote, O. Chamberlain, E. H. Rogers, H. M. Steiner, C. E. Wiegand and T. Ypsilantis, Phys. Rev. *122* (1961) 948.
[8] E. H. Rogers, O. Chamberlain, J. H. Foote, H. M. Steiner, C. Wiegand and T. Ypsilantis, Rev. Mod. Phys. *33* (1961) 356.
[9] P. J. Bussey, J. R. Carter, D. R. Dance, D. V. Bugg, A. A. Carter and A. M. Smith, Nucl. Phys. *B58* (1973) 363.

[10] V. A. GORDEEV, V. P. KOPTEV, S. P. KRUGLOV, L. A. KUZMIN, A. A. KULBARDIS, YU. A. MALOV, I. I. STRAKOVSKI and G. V. SCHERBAKOV, Academy of Sciences of the UdSSR, Leningrad Nuclear Physics Institute, 209, Leningrad (1976).
[11] A. A. CARTER, J. R. WILLIAMS, D. V. BUGG, P. J. BUSSEY and D. R. DANCE, Nucl. Phys. *B26* (1971) 445.
[12] D. DAVIDSON, T. BOWEN, P. K. CALDWELL, E. W. JENKINS, R. M. KALBACH, D. V. PETERSEN, A. E. PIFER and R. E. ROTHSCHILD, Phys. Rev. *D6* (1972) 1199.
[13] B. TROMBORG, S. WALDENSTRØM and I. ØVERBØ, Phys. Rev. *D15* (1977) 725.
[14] H. ZIMMERMANN, Helv. Phys. Acta *47* (1974) 130.